Proceedings of the ASME 2018 37th International Conference on Ocean, Offshore and Arctic Engineering
OMAE2018
June 17-22, 2018, Madrid, Spain

OMAE2018-78308

A COMPARISON STUDY ON THE HYDROELASTICITY OF TWO TYPES OF FLOATING BRIDGES IN INHOMOGENEOUS WAVE CONDITIONS

Shuai Li
State Key Laboratory of Ocean Engineering,
Shanghai Jiao Tong University
Shanghai, 200030 China

Shixiao Fu[1]
State Key Laboratory of Ocean Engineering,
Shanghai Jiao Tong University
Shanghai, 200030 China

Wei Wei
State Key Laboratory of Ocean Engineering,
Shanghai Jiao Tong University
Shanghai, 200030 China

Torgeir Moan
Centre for Ships and Ocean Structures (CeSOS),
Norwegian University of Science and Technology (NTNU), Trondheim, Norway
Department of Marine Technology,
NTNU, Trondheim, Norway

ABSTRACT

Due to the interaction between elastic structural deformations and fluid motions, the responses of floating bridges should be analyzed by hydroelasticity methods. We firstly employed a linear time-domain approach, based on the discrete-module-based hydroelastic method to investigate the responses of two surface bridge concepts under first order wave forces, a straight bridge with mooring system and an end-anchored curved bridge. The results show that the displacement of the curved bridge is smaller, compared with the straight bridge. However, the reaction force and the vertical bending moment of the curved bridge are larger. Furthermore, a nonlinear time-domain hydroelasticity approach for analysis of the floating bridge under nonlinear wave forces within inhomogeneous wave conditions is established. Finally, a comparison between the linear and nonlinear responses of the moored straight bridge is made. The results show that the nonlinearity of the wave excitation forces has a significant influence on the mooring forces and horizontal displacement.

***Key words**:* time-domain; nonlinear hydroelastic analysis; inhomogeneous wave conditions; surface bridge concepts

1. INTRODUCTION

The Norwegian Public Roads Administration (NPRA) is planning to build floating bridges for crossing the fjords on the E39 [1]. Due to the large water depth, the traditional undersea tunnels will be very expensive. Surface bridge concepts are supposed to be economically better in the crossing design of the fjord. The surface bridge concept mainly consists of pontoons and bridge girders. Two main alternatives of the pontoon supported floating bridge design concept are under consideration. One is a straight floating bridge with pre-tensioned mooring lines on the pontoons in their transverse direction. Another one is a curved bridge with only two ends constrained by the shores. Moreover, ocean wave condition is affected by the shores of fjords when propagating from the open sea, and then will become inhomogeneous along the length of the bridge, which may significantly change the response characters of the floating bridge under waves.

Distinguished from the traditional marine structures, floating bridges with a dimension of several kilometers will become quite flexible, which is known as very large floating structures (VLFS). With the huge size and relatively low structural stiffness, the responses of the VLFS in waves includes rigid body motions and structural deformations. Because of the strong coupling between structural deformations and fluid motions, the responses of the VLFS should be determined by means of hydroelasticity theories.

In the last several decades, frequency domain hydroelasticity theories have been developed from 2D[2] to 3D[3], from linear[4] to nonlinear theories[5,6], and applied to estimate

[1]Corresponding Author: Shixiao Fu, Tel: +86 13501947087; E-mail address: shixiao.fu@sjtu.edu.cn

responses of VLFS. The literature on hydroelasticity analysis of VLFS' is mainly restricted to homogeneous waves.

The floating structure is subjected to first order hydrodynamic force and second order force[7-9]. Based on the nonlinear hydroelasticity theory of Wu[8], Chen showed that the second order forces have a momentous effect on the horizontal displacement and mooring forces of a very large floating structure[4].

The second order forces can be decomposed into three parts, the steady component, the difference frequency component and the sum frequency component, calculated by the quadratic transform functions (QTFs). To solve the QTFs, three methods have been established, namely the far field approach[10], the middle field approach[11] and the near field approach[12].

The near field approach, based on the direct integration of the nonlinear second order pressure over wetted surface, can obtain six DOFs second order nonlinear wave forces of single or multi-body system.

Though the whole QTFs are preferable to investigate the effect of the second-order nonlinear forces, it is time-consuming and need large computation sources, which motivated the researchers to look for simplified methods. The well-known Newman's approximation[13] is widely used in the offshore industry. It uses the steady drift force transfer function, which has no contribution from the second-order potential and can be easily calculated with the linear panel method codes, to calculate the whole QTFs. This method could be used for difference frequency component of the second order wave loads.

The above researches about the nonlinear hydroelasticity are used on the assumption of linear mooring forces and homogeneous wave conditions. In this paper, based on the recently methods[14-16], a nonlinear time-domain hydroelastic method has been presented for floating bridges considering a nonlinear mooring system and inhomogeneous waves. The inhomogeneous wave filed is firstly described by several wave spectrums along the length of the bridge. The frequency-domain hydrodynamic coefficients of the floating pontoons are firstly calculated by panel method, and transformed into the time-domain using Cummins' equation. Furthermore, the time history of the first order wave excitation forces on each pontoon are calculated in terms of their spatial locations in the wave field. The difference frequency second order wave excitation forces on each pontoon are calculated by Newman's approximation as well. The stiffness properties of the mooring lines in the horizontal plan are simulated by nonlinear springs. Finally, the hydroelastic response of the two bridges are presented, including the displacement, internal structural forces, reaction forces and the mooring forces. The results show that the displacement of the curved bridge is smaller than the straight bridge, and the influence of nonlinear wave forces on the mooring system of the straight bridge cannot be neglected.

2. THEORETICAL BACKGROUND

2.1. Coordinate system

The bridge girder supported by pontoons, based on the hydrodynamic point of view, can be looked as a continuous beam connected multi-floating-body system. In this paper, three right-handed coordinate systems are used to describe the wave induced motions of the system, including global coordinate system $OXYZ$, reference coordinate system $o'_m x'_m y'_m z'_m$ and body-fixed coordinate system $o_m x_m y_m z_m$ ($m = 1,2,...M$), as illustrated by Fig. 1.

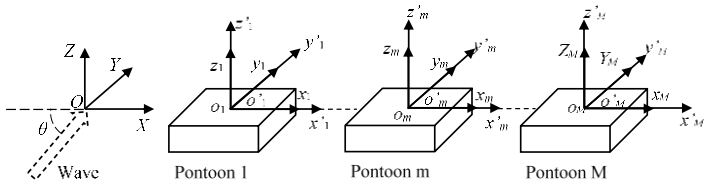

Fig. 1 Coordinate system of multi-floating-body system

2.2. Motion equations in time domain

Based on the present linear time-domain hydroelastic method [15,16], the floating bridge is considered as rigid pontoons connected by a elastic beam, as shown in Fig. 2. The dynamic motion equations in the global coordinate system can be expressed as follows,

$$\left[M+m+A(\infty)\right]_{6N\times 6N}\left\{\ddot{x}(t)\right\}_{6N\times 1}+\int_{-\infty}^{t}\left[H(t-\tau)\right]_{6N\times 6N}\left\{\dot{x}(\tau)\right\}_{6N\times 1}d\tau +\left[D\right]_{6N\times 6N}\left\{\dot{x}(t)\right\}_{6N\times 1}+\left[K+k\right]_{6N\times 6N}\left\{x(t)\right\}_{6N\times 1}=\left\{F_w^{(1)}(t)\right\}_{6N\times 1} \tag{1}$$

where $\left[M\right]$ is the mass matrix of the floating pontoons, $\left[m\right]$ is the mass matrix of the beam and $\left[A(\infty)\right]$ is the added mass coefficient matrix in the infinite wave frequency; $\left[H(t)\right]$ is the retardation function matrix, and its integral $\int_{-\infty}^{t}\left[H(t-\tau)\right]\left\{\dot{u}(\tau)\right\}d\tau$ represents the fluid memory effect; $\left[D\right]$ is the structural damping matrix of the beam; $\left[K\right]$ is the hydrostatic restoring coefficient, $\left[k\right]$ is the structural stiffness matrix of the beam; $\left\{F_w^{(1)}(t)\right\}$ is the first order time-domain wave exciting force; $\left\{x(t)\right\}$, $\left\{\dot{x}(t)\right\}$ and $\left\{\ddot{x}(t)\right\}$ are

the displacement, velocity and acceleration of the nodes with respect to the inertial reference frame respectively.

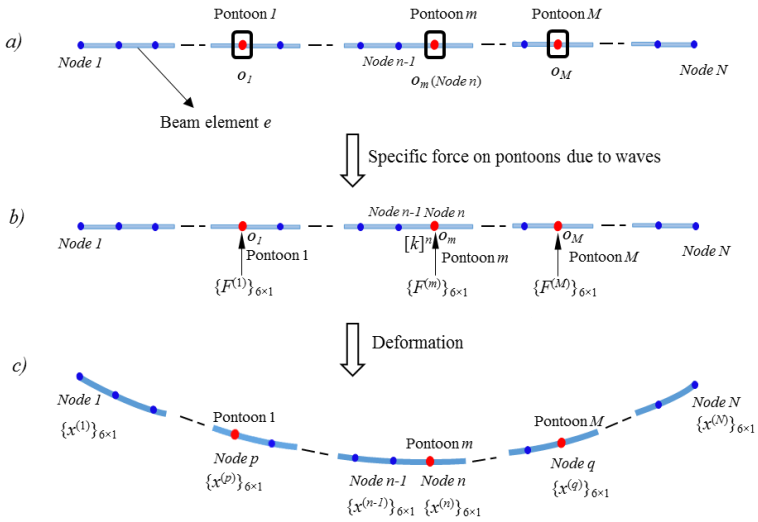

Fig. 2 The numerical method of the motion equation

2.3. Dynamic equations of nonlinear wave forces in inhomogeneous waves

2.3.1 Wave forces in inhomogeneous irregular waves

Considering the variation of the wave field along the floating bridge, the structure is firstly divided into different regions. The wave of each region is assumed homogeneous, as shown in Fig. 3.

According to three dimensional potential theory and linearized Bernoulli equation, the j^{th} order mode first order wave excitation force on the m^{th} pontoon within k^{th} region could be written as[15],

$$F_{mj}^{(1)}(t)=\sum_{l=1}^{L}\overline{f}_{j}^{(1)}(\omega_l,\theta)\sqrt{2S_k(\omega_l)\Delta\omega}\cos\left(\omega_l t+\varepsilon_l+\beta_j^{(1)}(\omega_l,\theta)\right) \tag{2}$$

where $F_{mj}^{(1)}$ is the j^{th} order mode first order wave excitation force on the m^{th} pontoon; $S_k(\omega_l)$ is the k^{th} wave spectrum; ω_l is the circular wave frequency; ε_l is the wave random phase; θ is the wave angle; $\overline{f}_j^{(1)}$ and $\beta_j^{(1)}$ are the amplitude and the phase angle of the first order wave excitation force.

Through the near field approach, introduced by Pinkster [9], we can obtain the j^{th} order mode difference frequency second order wave excitation force on the m^{th} pontoon within k^{th} region,

$$F_{mj}^{(2)}=\sum_{i=0}^{L}\sum_{l=1}^{L}\left(\begin{array}{l}\frac{1}{2}\sqrt{2S_k(\omega_i)\Delta\omega}\sqrt{2S_k(\omega_l)\Delta\omega}\left(T_{il}(\omega_i,\omega_l,\theta_k)\right)_j\times\\ \cos\left\{(\omega_i-\omega_l)t+(\varepsilon_i-\varepsilon_l)+\beta_j^{(2)}(\omega_i,\omega_l,\theta_k)\right\}\end{array}\right) \tag{3}$$

where $F_{mj}^{(2)}$ is the j^{th} order mode wave excitation force on the m^{th} pontoon; T_{il} and $\beta_j^{(2)}$ are the amplitude and phase angles of the difference frequency QTF (Quadratic Transfer Function); Other terms keep the same meanings as previous descriptions..

Since the calculation of the whole QTFs by the near field approach is relatively complicated and time-consuming, in this paper, Newman's approximation is adopted to obtain the whole QTFs of difference frequency component [13],

$$T_{il}(\omega_i,\omega_l)=\frac{1}{2}\left[T_{ii}(\omega_i,\omega_i)+T_{ll}(\omega_l,\omega_l)\right] \tag{4}$$

where T_{ii} and T_{ll} are the steady drift force transfer function of each pontoon, computed by the near field approach.

Consequently, the time history of the first order and the second order wave forces in an inhomogeneous wave condition can be written in the form of array,

$$\begin{aligned}\left\{F_w^{(1)}(t)\right\}&=\left\{...,\left\{F_{1,1}^{(1)}(t)\right\},...,\left\{F_{m,1}^{(1)}(t)\right\},...,\left\{F_{m,6}^{(1)}(t)\right\},...,\left\{F_{M,6}^{(1)}(t)\right\}...\right\}^T\\ \left\{F_w^{(2)}(t)\right\}&=\left\{...,\left\{F_{1,1}^{(2)}(t)\right\},...,\left\{F_{m,1}^{(2)}(t)\right\},...,\left\{F_{m,6}^{(2)}(t)\right\},...,\left\{F_{M,6}^{(2)}(t)\right\}...\right\}^T\end{aligned} \tag{5}$$

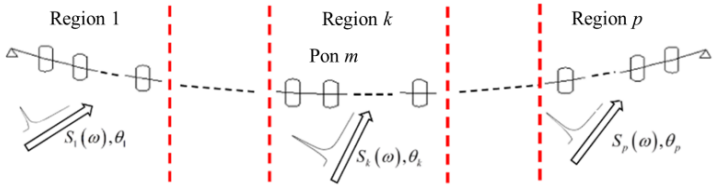

Fig. 3 The description of inhomogeneous sea environment

2.3.2 Motion equations of nonlinear wave forces in inhomogeneous waves

Based on the linear equations and the nonlinear second order wave excitation forces, considering the mooring system as well, the time-domain nonlinear hydroelastic equations of the beam can be expressed as,

$$\begin{aligned}&\left(\begin{array}{l}\left[M+m+A(\infty)\right]_{6N\times6N}\left\{\ddot{x}(t)\right\}_{6N\times1}+\int_{-\infty}^{t}\left[H(t-\tau)\right]_{6N\times6N}\left\{\dot{x}(\tau)\right\}_{6N\times1}d\tau+\\ \left[D\right]_{6N\times6N}\left\{\dot{x}(t)\right\}_{6N\times1}+\left[K+k\right]_{6N\times6N}\left\{x(t)\right\}_{6N\times1}+\left\{R(t)\right\}_{6N\times1}\end{array}\right)\\ &=\left\{F_w^{(1)}(t)\right\}_{6N\times1}+\left\{F_w^{(2)}(t)\right\}_{6N\times1}\end{aligned} \tag{6}$$

where $\left\{R(t)\right\}$ is the nonlinear restoring force of the mooring system, further written as,

$$\left\{R(t)\right\}=\left[K_m\right]\left\{x(t)\right\} \tag{7}$$

where $[K_m]$ is the equivalent nonlinear mooring stiffness.

Ultimately, the Eq(6) is numerically solved by Newmark method and the hydroelastic responses of the bridge under nonlinear forces in inhomogeneous can be obtained.

3. NUMERICAL MODEL

3.1 The curved floating bridge numerical model

A used pontoon supported floating bridge studied by Fu et al. [15] is as the numerical model of the curved bridge, with boundary conditions simplified to be simply-support, as shown in Fig.5.

The hydrodynamic model of the pontoon is showed in Fig.4. The connected beam with length of 196.96m, includes three different components. The properties of the first component (Section C1) are as same as the end component (Section C1). The middle component(Section C2) is 147.74m long. the main parameters of the segments and the pontoon are listed in Table. 1.

Table. 1 General Parameters of the Pontoon and the Curve Bridge Girder

	Properties	Number	
Bridge Girder	Section	C1	C2
	Length, L(*m*)	24.62	147.74
	EA (*kN*)	5.25E8	3.89E8
	EI_y ($kN*m^2$)	3.85E9	2.76E9
	EI_z ($kN*m^2$)	2.18E11	1.55E11
	GI_t ($kN*m^2$)	3.7E9	2.9E9
	Translation Mass (*te/m*)	31.8	26.71
	Rotation Mass ($te*m^2/m$)	10507	8118
Pontoon	Length (*m*)	62	
	Width (*m*)	22	
	Draft (*m*)	10.5	

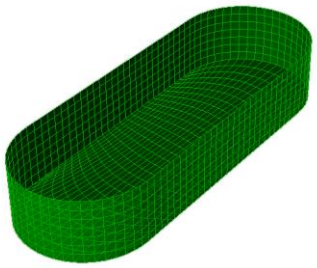

Fig. 4 Hydrodynamic Meshes of the Floating Pontoon

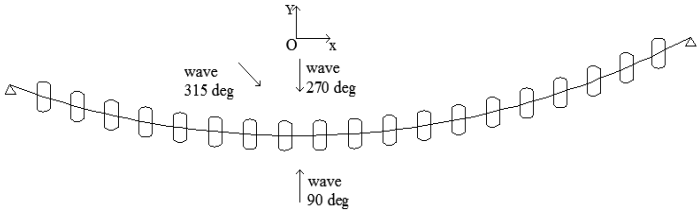

Fig. 5 Simplified model of the curved floating bridge

3.2 The straight floating bridge numerical model

Similar to the curved bridge, the straight bridge also consists of 19 pontoons and a continuous bridge girder. The two ends of the bridge are also simplified as pin joints, as illustrated in Fig. 6. The pontoons of the straight bridge are the same with the curved bridge. The connected beams also consist of three segments with different cross sections. The length of the each segment is 25m(Section S1), 153m(Section S2) and 25m(Section S1) respectively. The main parameters of the straight bridge girder are listed in Table 2 。

Table. 2 General Parameters of the Straight Bridge Girder

	Properties	Number	
Straight Bridge Girder	Section	S1	S2
	Length, L(*m*)	25	153
	EA (*kN*)	4.64E8	153
	EI_y ($kN*m^2$)	3.79E9	3.26E8
	EI_z ($kN*m^2$)	3.88E10	2.68E9
	GI_t ($kN*m^2$)	4.61E9	2.65E10
	Translation Mass (*te/m*)	24.92	3.20E9
	Rotation Mass ($te*m^2/m$)	Neglected	19.69

Different from the curved bridge, the straight bridge requires mooring systems to maintain the stability itself. The position of the mooring lines are located on the 3rd, 9th and 15th pontoons respectively, shown in Fig. 6.

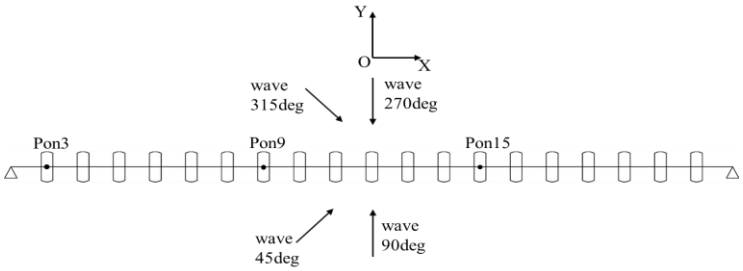

Fig. 6 Simplified model of the straight floating bridge

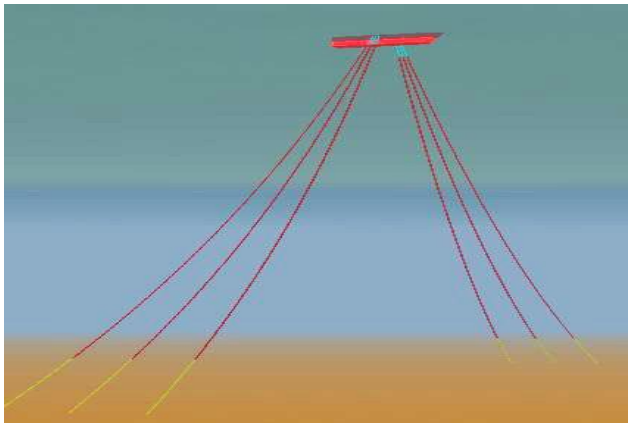

Fig. 7 Model of the mooring system

As illustrated by Fig. 7, each mooring system is composed of six same mooring lines, whose main parameters are summarized in Table. 3. Pretension load on the tethers of 3rd, 9th and 15th pontoons is 800kN, 3800kN and 4200kN respectively.

Table 3 Mooring line component properties

Properties	Bottom anchor -chain	Cable	Top anchor-chain
Diameter(*mm*)	175	175	175
Axial Stiffness(*kN*)	2.41×10^6	1.59×10^6	2.61×10^6
Minimum Breaking Load (*kN*)	25200	24300	27900
Dry Mass (*kg/m*)	685	203	783
Normal Drag Coefficient	3.5	3.0	4.6
Axial Drag Coefficient	1.7	0.01	2.2
Length,(*m*) （Pon3, 9）	100	641	20
Length,(*m*) (Pon15)	100	920	20

4. RESULTS AND DISCUSSION

4.1. Linear responses of the straight and curved floating bridge in inhomogeneous irregular waves

In the present study, the inhomogeneous wave field is firstly divided into 4 regions. The irregular waves in each region is simulated by a JONSWAP spectrum. The main parameters are displayed in Table 4 and Fig 8.

Table 4 Wave Parameters at each region along the bridge length [18]

Env. Number	Regions(from West to East)	Significant wave height(H_s/m)	Peak period(T_p/s)
Env.1	Region A (0-1km)	2.0	5
Env.2	Region B (1-2km)	1.9	6
Env.3	Region C (2-3km)	2.4	7.5
Env.4	Region D (3-4km)	2.8	8.5

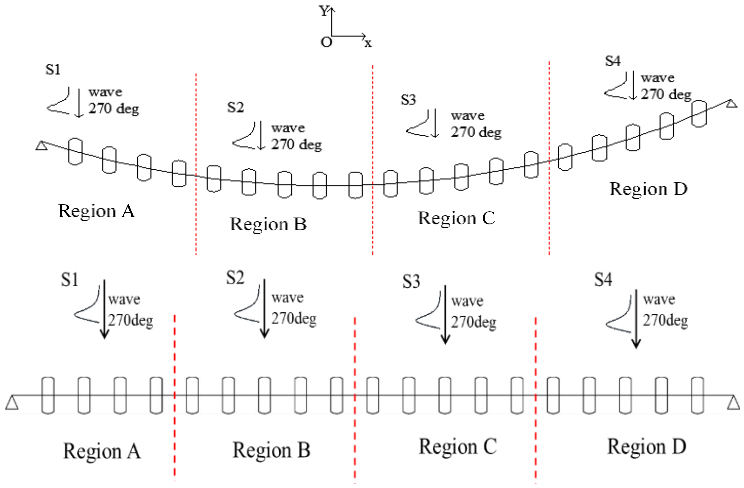

Fig. 8 Distribution of inhomogeneous wave field in fjord

Fig. 9 illustrates the comparative significant values of the vertical displacement, horizontal displacement and torsional angle along the longitudinal direction for the straight and curved bridge, under the inhomogeneous wave and the homogeneous waves (S4), with the wave direction of 270°. As shown in the figure, the boundaries between the regions have been marked by lines.

The vertical displacement of the curved bridge is smaller than the straight bridge, however, the maximum of the two bridges are almost equal. As for the horizontal displacement, the peak value of the straight bridge is far larger than that of the curved bridge, especially in inhomogeneous waves, where the maximum of the straight bridge is almost three times greater than that of the curved bridge. Due to the different structural characteristics of the two bridges, the maximum value of the straight bridge appears in region D and the appearance of the curved bridge's maximum is in region B, in inhomogeneous waves. The torsional angles of the curved bridge is always smaller than that the straight one, in both homogeneous and inhomogeneous waves.

Accordingly, for the wave direction of 270°, the displacement of the curved floating bridge is smaller than that of the straight floating bridge.

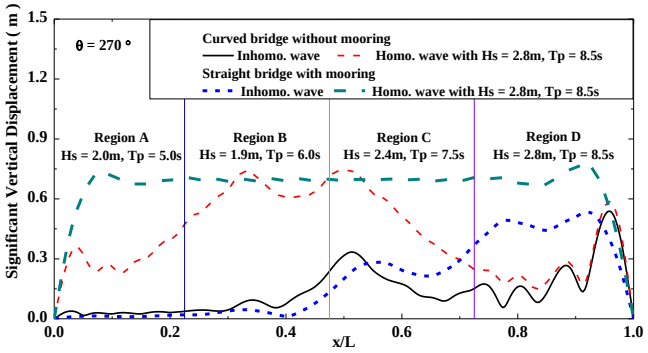

(a) Vertical displacement

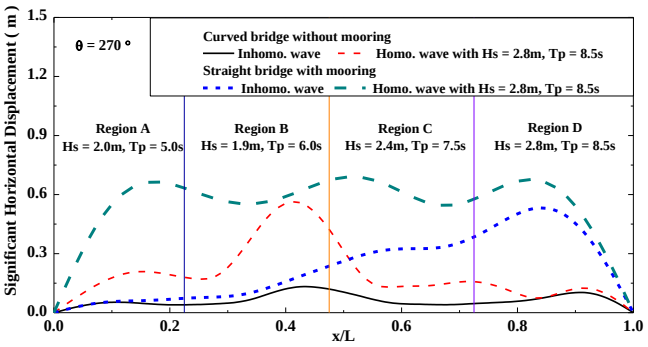

(b) Horizontal displacement

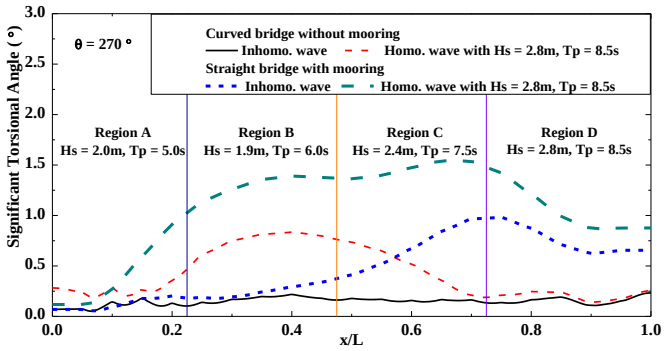

(c) Torsional angle

Fig. 9 The significant displacements of the straight and curved bridge along the longitudinal direction in the homogenous and inhomogeneous waves (θ=270°)

The distribution of the vertical bending moment, horizontal bending moment and torsional moment along the two bridges are illustrated in Fig. 10.

The vertical bending moment of the curved bridge is invariably greater than that of the straight bridge, in both homogeneous and inhomogeneous waves. And the maximum of the curved bridge is approximately 1.5 times and 3 times as much as those of the straight bridge, in both homogeneous and inhomogeneous waves respectively.

On the other hand, the maximum horizontal bending moment of the straight bridge is nearly four times that of the curved bridge, no matter in homogeneous waves or inhomogeneous waves. When the wave is incident along the bridge radian in the direction of 270°, the curvature of the bridge may counteract some horizontal bending moment, causing that the curved bridge's value is much smaller than the straight bridge's.

With regards to the torsional moment, the results on Fig.10(c) show that the peak values of the two bridges appear on region A in homogeneous wave conditions, where the maximum of the curved bridge is slightly larger than that of the straight bridge. In inhomogeneous waves, the maximum of the two bridges are approximately equal, but the positions of them are different. The maximum values of the straight bridge and the curved bridge appear in the region C and A, respectively.
Thus, compared with the straight bridge, the vertical bending moment of curved floating bridge is relatively larger, but the horizontal bending moment is smaller. The torsional moment of the two structures is not much different.

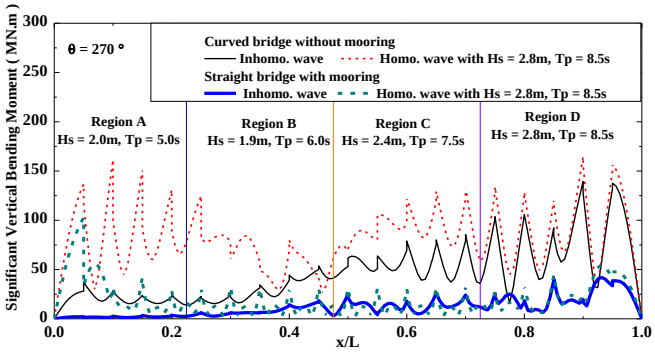

(a) Vertical bending moment

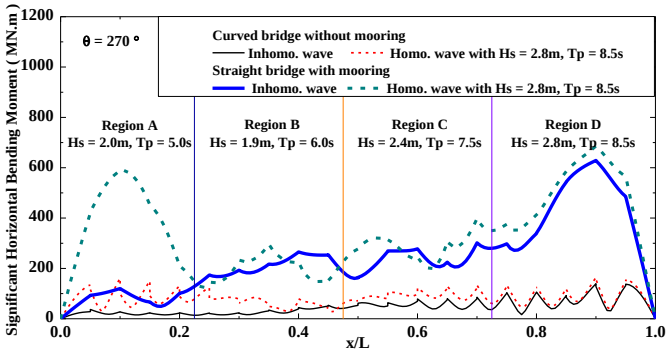

(b) Horizontal bending moment

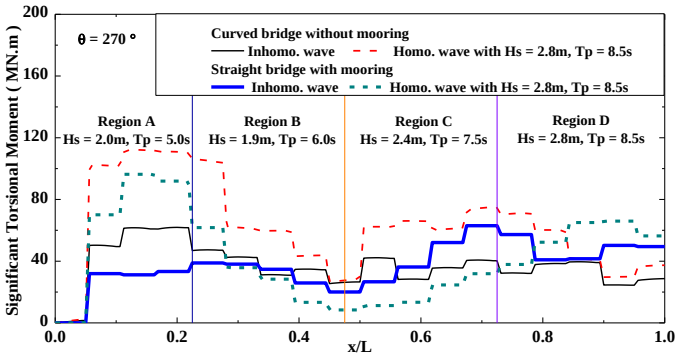

(c) Torsional moment

Fig. 10 The significant forces of the straight and curved bridge along the longitudinal direction in the homogenous and inhomogeneous waves (θ=270°)

The significant reaction forces of the two floating bridges are shown in Table 5. The reaction forces of the curved bridge are invariably greater than those of the straight bridge, the difference of the force along the x-axis direction is the most obvious. Especially in the homogeneous waves, the reaction force of the right end of the curved bridge along the x-axis is about 30 times that of the straight one.

Table 5 The reaction force for the wave direction of 270°

Bridge type	Curved		Straight	
Reaction force (MN)	Inhomogeneous wave	Homogeneous wave S_4	Inhomogeneous wave	Homogeneous wave S_4
F_x_*Left*	3.795	11.061	0.379	1.733
F_y_*Left*	1.206	3.861	0.495	2.265
F_z_*Left*	0.229	0.918	0.022	0.730
F_x_*Right*	2.929	12.769	0.180	0.413
F_y_*Right*	2.892	5.049	2.545	2.947
F_z_*Right*	0.995	1.090	0.382	0.465

4.2. Nonlinear responses of straight floating bridge in inhomogeneous irregular waves

Since the difference frequency second order force has a significant effect on the horizontal displacement and the mooring system, it is necessary to analyze the nonlinear hydroelastic responses of the straight floating bridge with mooring system, under nonlinear wave excitation forces.

Fig. 11 presents the comparisons of the time history of vertical displacements, under the combined first and second order, only the first order and only the second order wave excitation forces in the wave direction of 45°, in inhomogeneous waves. The vertical displacements under the combined first and second order and only the first order wave excitation force are mostly the same, that is, the influence of the second order nonlinear wave forces on the vertical displacement is not significant.

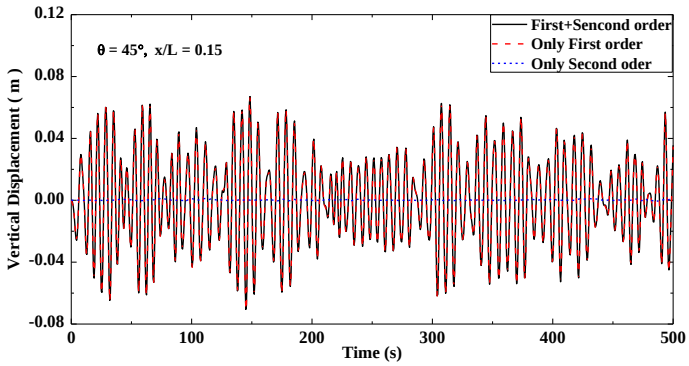

(a) Position, x/L=0.15

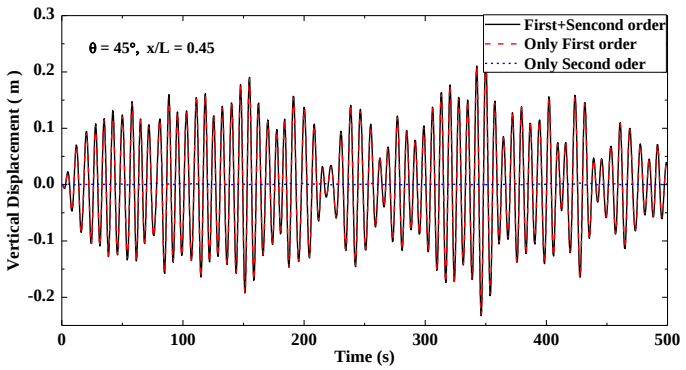

(b) Position, x/L=0.45

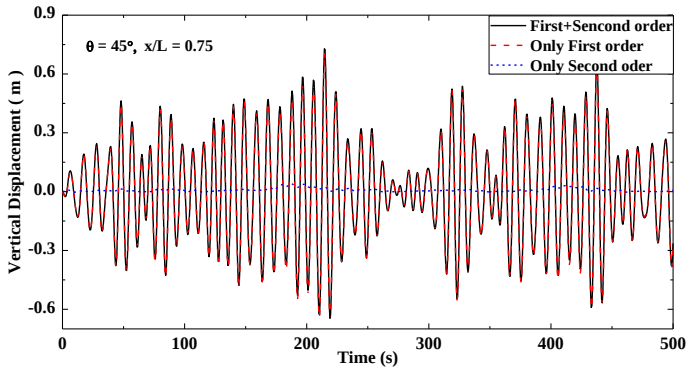

(c) Position, x/L=0.75

Fig. 11 Time history of the vertical displacement in different positions along the bridge (θ=45°)

As illustrated in Fig.12, the statistical results of the horizontal displacement time history are along the bridge include the mean, maximum, minimum and standard deviation, under the linear(only the first order wave excitation force) and nonlinear wave forces (the combined first and second order wave excitation force).

Only under the first order linear wave excitation force, the average value of the horizontal displacement is almost zero. Compared with the linear results, the bridge has obvious deviation along the wave direction, especially in the middle part of the bridge (x/L=0.5), because of the second order

nonlinear wave force component. The maximum and standard deviation under the nonlinear wave excitation force are nearly three times those under the first order force, and the minimum value is approximately twice that under the linear forces, as we can see from Fig. 12(b) ~(d).

Owing to the inhomogeneity of the waves, the peak values of the maximum, the minimum and the standard deviation curves appear in the region D(x/L=0.75~1.0) with the largest waves.

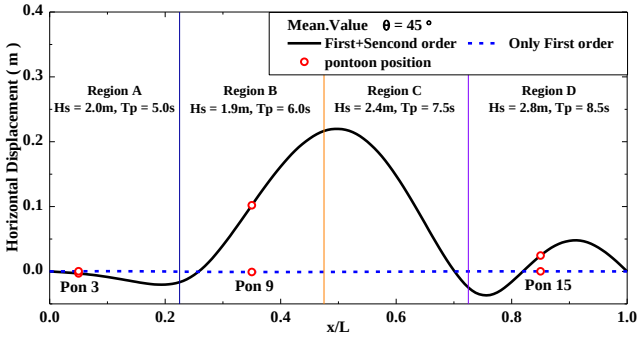

(a) Mean

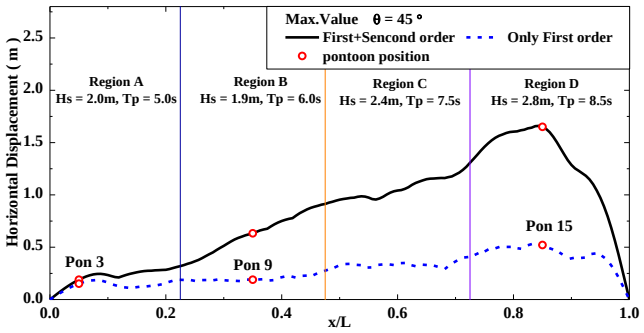

(b) Maximum

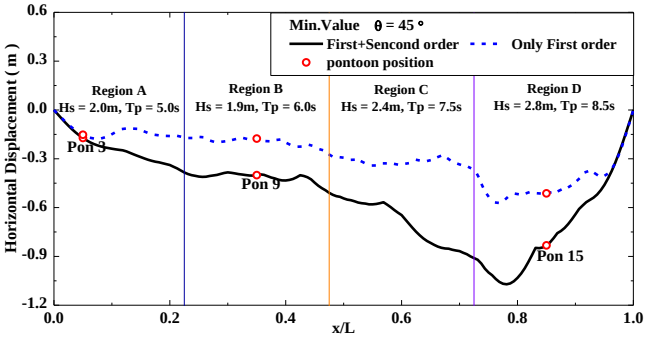

(c) Minimum

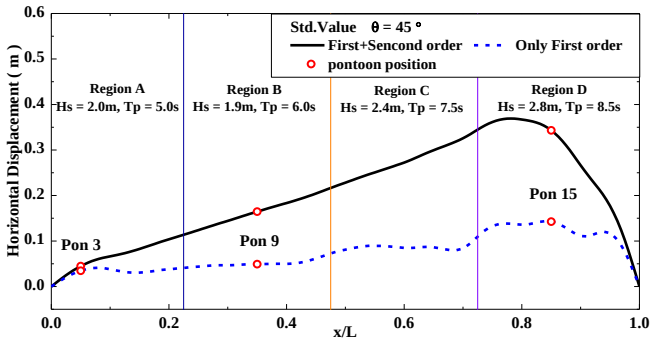

(d) Standard deviation

Fig. 12 Response statistic of the horizontal displacements under linear (only first order) and nonlinear (first+second order) wave excitation forces.

Under the combined first and second order, only the first order and only the second order wave excitation forces, the mooring forces of the mooring system on the three Pontoons are shown in Fig. 13.

The mooring force under the nonlinear wave force, is far larger than that under the first order linear wave excitation force. Distinguished from the long-period motion of the mooring force only under the second order wave force, the oscillation of the wave frequency exists in the mooring force, under the nonlinear wave force.

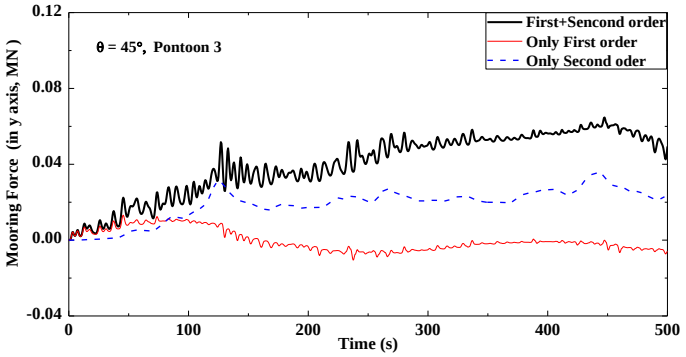

（a）Pontoon 3

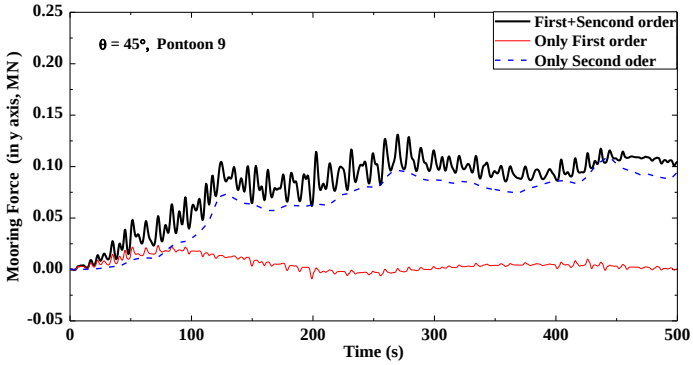

（b）Pontoon 9

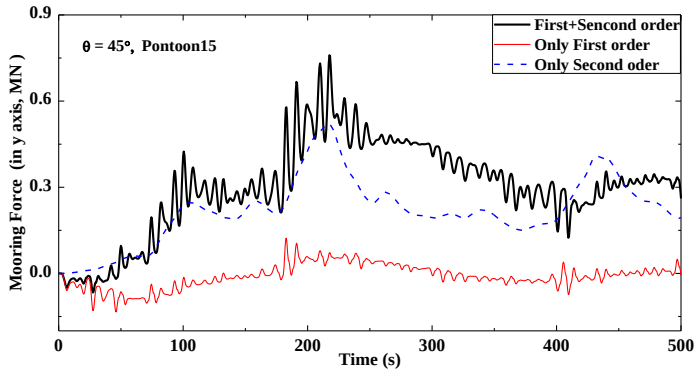

（c）Pontoon 15

Fig. 13 Time history of the mooring force on different pontoons (θ=45°)

To further analyze the influence of the second order wave excitation force on mooring system, Table 6 summarizes the statistical results of the mean, maximum, minimum and standard deviation of the mooring force, under the nonlinear and linear wave forces.

The mean mooring force is not zero due to the second order component of wave excitation forces. For the pontoon 9 and the pontoon 15, the maximum amplitude of the mooring force is much larger than the minimum amplitude under nonlinear wave forces, which are 4.5 times and 16 times of the minimum respectively. Different from the 9th and 15th pontoon, the maximum and minimum amplitude of 3rd pontoon are nearly equal, which is consistent with the pontoon motions shown in Fig. 12.

Table 6 The mooring force for the wave direction of 45°

Pontoon number	Wave force	Mean (MN)	Maximum (MN)	Minimum (MN)	Standard deviation (MN)
Pon3	Nonlinear	-0.030	0.053	-0.087	0.027
	Linear	-0.001	0.008	-0.013	0.002
Pon9	Nonlinear	0.150	0.253	0.054	0.014
	Linear	0.001	0.025	-0.016	0.002
Pon15	Nonlinear	0.430	1.530	-0.088	0.178
	Linear	0.000	0.113	-0.135	0.017

Moreover, the statistical results of the three component reaction forces are listed in Table 7. As can be seen, nonlinear wave force has little effect on the support reaction force. Compared with the mooring system, the support is primarily subjected to the first order wave force, while the magnitude of the second order wave force is far smaller than the linear force. Therefore, under the linear wave force or nonlinear wave force, The reaction forces are little difference.

Table 7 The reaction force for the wave direction of 45°

	Wave force	Mean (MN)	Maximum (MN)	Minimum (MN)	Standard deviation(MN)
Fx_Left	Nonlinear	-0.302	10.776	-10.355	2.722
	Linear	0.000	11.053	-9.806	2.692
Fy_Left	Nonlinear	-0.009	0.684	-0.644	0.170
	Linear	0.000	0.693	-0.652	0.169
Fz_Left	Nonlinear	-0.003	0.675	-0.675	0.169
	Linear	0.000	0.679	-0.678	0.169
Fx_Right	Nonlinear	-0.520	26.008	-28.101	0.665
	Linear	0.000	28.282	-26.618	0.636
Fy_ Right	Nonlinear	-0.101	3.349	-3.885	1.031
	Linear	0.000	3.567	-3.690	1.026
Fz_ Right	Nonlinear	0.001	2.176	-2.068	0.605
	Linear	0.000	2.157	-2.072	0.606

5. CONCLUDING REMARKS

A linear time-domain hydroelastic method is adopted to investigate the responses of two floating bridges. The comparisons of the displacement shows that the deformation of the curved bridge is smaller than the straight bridge. While as for the structural forces, compared with the straight bridge, the vertical bending moment and reaction forces of the curved are much larger.

The straight bridge with mooring system is investigated by using the first and second order for horizontal wave load, considering difference frequency components. The mooring is represented by equivalent nonlinear spring stiffness. The results indicate that the second order components play a dominant role on the mooring forces and horizontal displacements.

The present study is limited in time and can be refined by investigating how the displacement of the straight bridge can be reduced by the mooring system, and how the bending moment in the two concepts can be reduced. Moreover, only one mean wave direction and limited amplitude are considered. More condition need to be considered to determine the design value of the response.

REFERENCE

[1] Xiang, X., Eidem, M.E., Sekse, J.H., Minoretti, A., 2016. Hydrodynamic loads on a submerged floating tube bridge induced by a passing ship or two ships in maneuver in calm water, ASME 2016 35th International Conference on Ocean, Offshore and Arctic Engineering. American Society of Mechanical Engineers.

[2] Bishop RE, Price WG. Hydroelasticity of ships: Cambridge University Press; 1979.
[3] Wu, Y., 1984. Hydroelasticity of floating bodies. University of Brunel.
[4] Wu, Y., Wang, D., Riggs, H. R., &Ertekin, R. C., 1993. Composite singularity distribution method with application to hydroelasticity. Marine Structures, 6(2-3), 143-163.
[5]Chen X, Wu Y, Cui W, Tang X. Nonlinear hydroelastic analysis of a moored floating body. Ocean Engineering. 2003;30:965-1003.
[6] Chen, X., Moan, T., Fu, S., & Cui, W., 2006. Second-order hydroelastic analysis of a floating plate in multidirectional irregular waves. International Journal of Non-Linear Mechanics, 41(10), 1206-1218.
[7] Ogilvie TF. Second order hydrodynamic effects on ocean platforms. Int Workshop on Ship and Platform Motions, 1983: University of California; 1983.
[8] Wu Y, Maeda H, Kinoshita T. The second order hydrodynamic actions on a flexible body. Journal of Institute of Industrial Science, University of Tokyo. 1997;49:8-19.
[9] Maeda H, Ikoma T, Masuda K, Rheem C-K. Time-domain analyses of elastic response and second-order mooring force on a very large floating structure in irregular waves. Marine structures. 2000;13:279-99.
[10] Maruo H. The drift of a body floating in waves. J Ship Res. 1960;4:1-10.
[11] Chen X-B. Middle-field formulation for the computation of wave-drift loads. Journal of Engineering Mathematics. 2007;59:61-82.
[12] Pinkster JA. Low frequency second order wave exciting forces on floating structures. 1980.
[13] Newman JN. Second-order, slowly-varying forces on vessels in irregular waves. 1974.
[14] Wei W, Fu S, Moan T, Lu Z, Deng S. A discrete-modules-based frequency domain hydroelasticity method for floating structures in inhomogeneous sea conditions. Journal of Fluids and Structures. 2017;74:321-39.
[15] Fu, S., Wei, W., Ou, S., Moan, T., Deng, S., Lie, H.,2017. A Time-domain Method for Hydroelastic Analysis of Floating Bridges in Inhomogeneous waves. 36th OMAE, Trondheim, 2017, Paper No. OMAE2017-62534
[16] Wei W, Fu S, Moan T, Song C, Ren T. A time-domain method for hydroelasticity of very large floating structures in inhomogeneous sea conditions. Marine Structures. 2018;57:180-92.
[17] Faltinsen, O.. Sea loads on ships and offshore structures. Cambridge University Press, Cambridge, UK.
[18] Lie, H., Fu, S., Fylling, I., Fredriksen, A. G., Bonnemaire, B., and Kjersem, G. L., "Numerical Modelling of Floating and Submerged Bridges Subjected to Wave, Current and Wind," Proc. ASME 2016 35th International Conference on Ocean, Offshore and Arctic Engineering, American Society of Mechanical Engineers, pp. V007T006A075-V007T006A075.